

## Use of the second-derivative differential thermal curve in the evaluation of cement–quartz pastes with metakaolin addition autoclaved at 180°C

Danielle S. Klimesch<sup>a,b</sup>, Abhi Ray<sup>b,\*</sup>

<sup>a</sup> James Hardie and Coy Pty Limited, 1 Grand Avenue, Camellia, P.O. Box 219, Granville, Sydney, NSW 2142, Australia

<sup>b</sup> Department of Materials Science, University of Technology, Sydney, P.O. Box 123, Broadway, Sydney, NSW 2007, Australia

Received 5 March 1997; received in revised form 22 August 1997; accepted 22 September 1997

### Abstract

A combination of DTA and the second-derivative differential thermal curve is a powerful technique in the evaluation of phases present in complex systems. An autoclaved cement-based system with metakaolin addition was used to demonstrate the importance of the second-derivative differential thermal curve in the detection of overlapping peaks and weak endothermic deflections. © 1997 Elsevier Science B.V.

**Keywords:** Autoclaving; Calcium silicate hydrates; Cement-quartz; Metakaolin; Second-derivative DTA

### 1. Introduction

Metakaolin (MK) is a reactive aluminosilicate which is formed by the dehydroxylation of kaolin precursor upon heating in the ~700–800°C temperature range [1]. It is well known that the addition of reactive aluminium-containing compounds accelerates the formation of tobermorite (C<sub>5</sub>S<sub>6</sub>H<sub>5</sub>) which is one of the most important strength-contributing calcium silicate hydrate binding phases occurring in autoclaved cured cement and/or lime-based building products [2]. Aluminium (Al) ions substitute for silicon (Si) ions to a maximum Al/Al+Si ratio of 0.14 [3]; higher Al concentrations in the mix result in the formation of hydrogarnets of variable composition which do not contribute much to the strength [4,5].

Previous studies, using DTA, of autoclaved cement-quartz pastes with kaolin and MK additions have suggested that MK is more reactive than the parent kaolin [6]. The absence of the mullite transformation exotherm above ~1000°C, for samples made with up to 40% MK suggested that MK had fully reacted [6]. From our own investigations of autoclaved cement-quartz–MK pastes, with MK additions of up to 30.5%, we have shown that there is an upper limit beyond which MK does not fully react [7]. Of particular interest is the ~800–1000°C region, which can be extremely complex and difficult to interpret, due to the presence of multiple effects resulting in peak overlap. Additionally, decreasing amounts of calcium silicate hydrates and hydrogarnets present in the sample result in a reduced signal, rendering their detection more difficult.

While DTA has been extensively used in the study of cement-based systems [5,6], information on the use of the second-derivative differential thermal curve

\*Corresponding author. Tel.: 00 61 2 330 1990; fax: 00 61 2 330 1551; e-mail: A.Ray@uts.edu.au

appears to be lacking. The present paper illustrates the use of DTA and, in particular, that of the second-derivative differential thermal curve (2nd deriv. DTA), in the study of autoclaved cement–quartz–MK pastes, when MK is introduced as either quartz or cement replacement. Our investigation demonstrates how the second-derivative differential thermal curve has been successfully employed in:

1. detecting overlapping peaks;
2. determining peak maxima of overlapping peaks; and
3. detecting weak endothermic deflections.

## 2. Experimental

Details of raw materials, mix proportions and curing regimes have been given elsewhere [7]. Briefly, cement–quartz pastes were prepared using ordinary Portland cement (61.5%) and ground quartz (38.5%), the bulk mol CaO/SiO<sub>2</sub> (C/S) ratio (0.83) constituting that of C<sub>5</sub>S<sub>6</sub>H<sub>5</sub>. MK was added at 6, 12, 18.25, 24 and 30.5% as quartz replacement in one series and as cement replacement in a second series. Water-to-

total-solids ratio was 0.46 for all mixes. Samples were autoclaved at 180°C for 8 h after an initial 24 h precure. Oven-dried, disc-milled specimens were analyzed using a TA-instrument SDT 2960 simultaneous DTA/TGA analyzer at a heating rate of 10°C/min to 1100°C under flowing nitrogen (100 ml/min). Sample sizes were between 40 to 45 mg and were packed into a Pt–Rh crucible with 20 taps. All curves were analyzed using the TA-instruments DTA-TGA data analysis software, which enables DTA, first- and second-derivative DTA curves to be evaluated. X-ray diffraction (XRD) using  $\theta$ – $\theta$  geometry (Siemens D-5000) was carried out using CuK $\alpha$  radiation for all specimens.

## 3. Results and discussion

### 3.1. DTA curves

Figs. 1 and 2 are DTA curves of autoclaved cement–quartz–MK samples, when MK was introduced as quartz and as cement replacement, respectively. Two-point rotations were employed for all DTA curves as described previously [8].

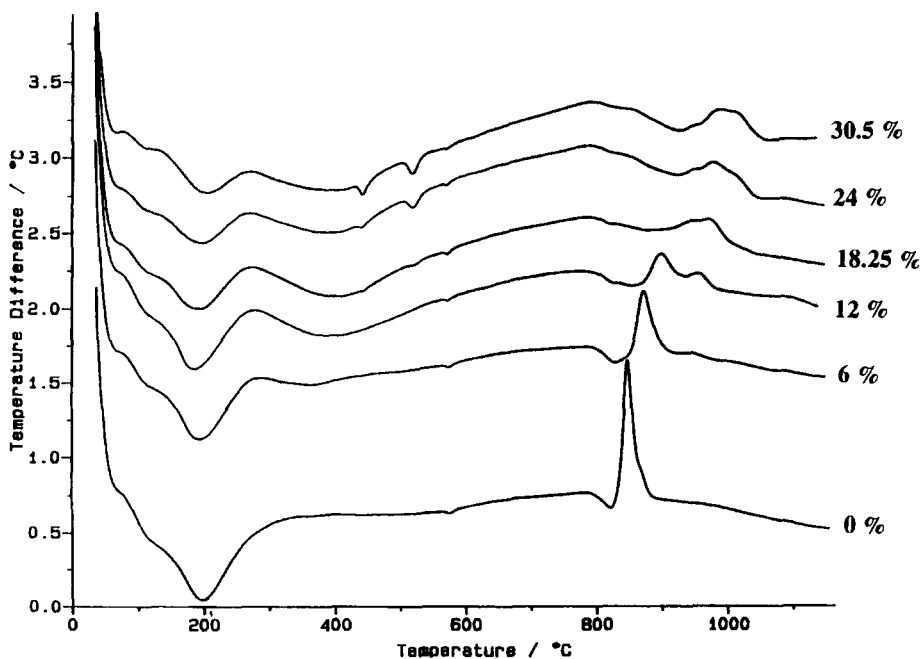


Fig. 1. DTA curves of autoclaved cement–quartz–MK pastes with increasing amounts of MK introduced as quartz replacement.

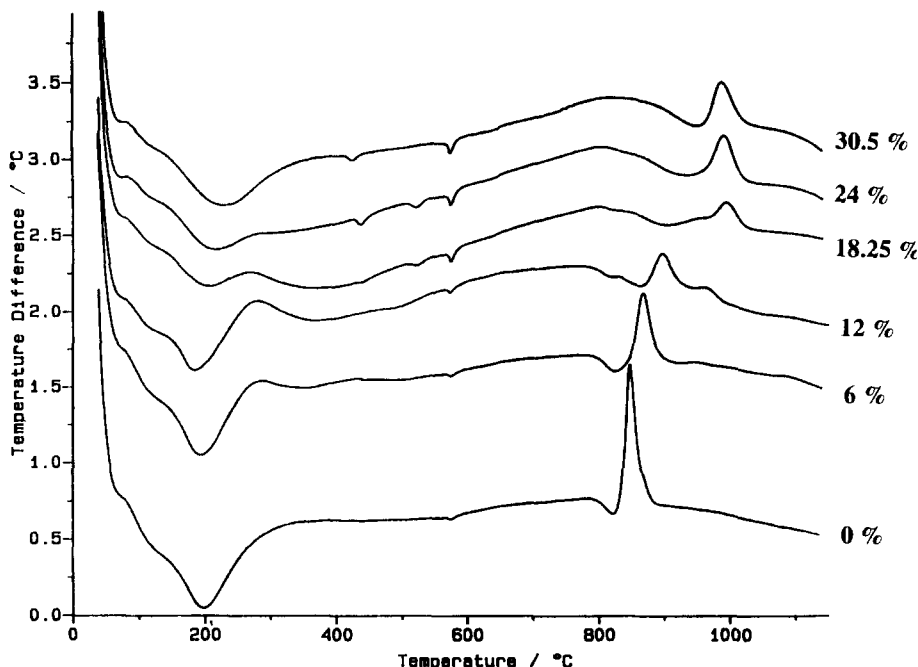


Fig. 2. DTA curves of autoclaved cement-quartz-MK pastes with increasing amounts of MK introduced as cement replacement.

### 3.1.1. MK introduced as quartz replacement

From Fig. 1 the following is apparent:

- Dehydration of calcium silicate hydrates is manifested by endotherms at  $\sim 130^\circ$  and  $\sim 200^\circ\text{C}$ , the latter shifting to a slightly higher temperature and decreasing in size with increasing MK addition. The small endotherm, below  $\sim 100^\circ\text{C}$ , present in all samples, is most likely due to moisture adsorbed during sample preparation for thermal analysis.
- The broad endotherm centred at  $\sim 360^\circ\text{C}$ , due to the dehydration of hydrogarnet,  $\text{C}_3\text{ASH}_4$ , increased in size with increasing MK addition. This endotherm appeared constant at 24 and 30.5% MK additions.
- The presence of portlandite, CH, and  $\alpha$ -dicalcium silicate hydrate,  $\alpha\text{-C}_2\text{SH}$ , is indicated by endotherms at  $\sim 445^\circ$  and  $\sim 525^\circ\text{C}$ , respectively. The endotherms increased in size with increasing MK used.
- The endotherm at  $\sim 575^\circ\text{C}$ , due to the crystalline inversion of unreacted quartz, remained fairly constant throughout this series. A slight decrease, however, is apparent for the sample made with 30.5% MK.

- The exotherm at  $\sim 840\text{--}900^\circ\text{C}$ , due to wollastonite formation from the dehydration residues of calcium silicate hydrates, CSHs, displays an increase in temperature and a reduction in height indicating increasing amounts of Al-substitution into the CSH lattice. The exotherm at  $\sim 940\text{--}980^\circ\text{C}$ , due to the formation of anorthite from the hydrogarnet dehydration residue, increased in height and temperature with increasing MK used. These observations are in accordance with previous findings [9,10].

The most striking feature in this series of samples, is a distinctive shift of exotherms from  $\sim 800\text{--}900^\circ\text{C}$  to the  $\sim 900\text{--}1000^\circ\text{C}$  region at and above 18.25% MK addition, and the concurrent appearance and increase of the  $\alpha\text{-C}_2\text{SH}$  phase. Additionally, the broadness and “bumpiness” of the exotherms indicate the presence of several overlapping effects, which are discussed under “2nd deriv. DTA curves”.

### 3.1.2. MK introduced as cement replacement

From Fig. 2, similar trends are apparent as in Fig. 1 with the following exceptions:

- The dehydration endotherm at  $\sim 200^\circ\text{C}$  decreased in size and shifted to slightly higher temperatures with increasing MK used, except for the specimen made with 30.5% MK, which showed an increase in the endotherm area.
- The broad endotherm at  $\sim 360^\circ\text{C}$  increased up to 18.25% MK addition, and then decreased. The distinctive flattening, particularly at 30.5% MK addition, indicates the possible absence of hydrogarnet. This trend was confirmed by XRD. The integrated intensity of the  $5.05 \text{ \AA}$  peak, due to  $\text{C}_3\text{ASH}_4$ , decreased at 24% MK addition and was hardly discernible at 30.5% MK addition.
- Endotherms at  $\sim 445^\circ\text{C}$  and  $\sim 525^\circ\text{C}$  increased in size with increasing MK used. The sample prepared with 30.5% MK, however, did not contain the  $\alpha\text{-C}_2\text{SH}$  phase.
- The amount of unreacted quartz increased with increasing MK addition as shown by the increase in size of the endotherm at  $\sim 575^\circ\text{C}$ . This indicates that decreasing amounts of quartz had reacted during autoclaving. A distinctive break in this trend is apparent at 18.25% MK addition and above, the unreacted quartz contents being more prominent at these additions.
- Incorporation of Al into the CSH crystal lattice is indicated by the increase in exotherm temperature, from  $\sim 840^\circ$  to  $\sim 900^\circ\text{C}$ , and decrease in height, while the exotherm due to anorthite formation increased in height and temperature, as noted previously.

As for Fig. 1, a distinctive shift of the exotherms to  $\sim 900\text{--}1000^\circ\text{C}$  at 18.25% MK addition and above is evident, but without similar broadening and “bumpiness”. This is particularly noticeable for samples made with 24 and 30.5% MK. Additionally, endotherms due to CH and  $\alpha\text{-C}_2\text{SH}$  were present and increased in size, while the second endotherm was absent at 30.5% MK addition.

A more detailed account of the effects on physical properties in relation to the phases present, with MK addition, has been given elsewhere [11].

### 3.2. 2nd deriv. DTA curves

Closer inspection of the DTA curves, however, reveals more detail than is at first apparent. Use

was made of the 2nd deriv. DTA curve to identify overlapping peaks, determine peak maxima and detect small endothermic deflections. This is illustrated by several examples, which also highlight the increasing complexity of the  $\sim 800\text{--}1000^\circ\text{C}$  region with increasing MK used.

*Example 1:* From Fig. 3, the DTA curve indicates that this exotherm may be due to two effects, at  $\sim 850^\circ$  and  $\sim 870^\circ\text{C}$ , while the 2nd deriv. DTA curve confirms it. The wollastonite formation is due to different precursor phases, namely Al-substituted tobermorite and CSH, with main  $d$ -spacings at 7.3 and  $3.04 \text{ \AA}$  for the latter, and has been referred to as “fibrous CSH” in earlier studies [12].

*Example 2:* Fig. 4 indicates three exotherms at  $\sim 840^\circ$ ,  $\sim 903^\circ$  and  $\sim 960^\circ\text{C}$ , which are due to the formation of wollastonite from CSH, Al-substituted tobermorite and that of anorthite from the hydrogarnet dehydration residue, respectively. The small endothermic deflection,  $\sim 828^\circ\text{C}$ , preceding the first small exotherm is probably due to well-crystallized calcite [13], and was present in nearly all samples. It should be noted that even though the signal intensity was much weaker than for the previous example, in accordance with the effects of increasing Al-content in the CSH lattice and its effect on the exotherm temperature and height, the 2nd deriv. DTA curve clearly separates these effects, thus allowing more accurate determinations of peak maxima than from the corresponding DTA curve.

*Example 3:* Fig. 5 displays an even more complex set of exotherms. The broad exotherm between  $\sim 900\text{--}1000^\circ\text{C}$  is clearly due to multiple effects as shown by the 2nd deriv. DTA curve which reveals exotherms at  $\sim 953^\circ$ ,  $\sim 982^\circ$  and  $1020^\circ\text{C}$ . The region between  $\sim 800\text{--}900^\circ\text{C}$  is more difficult to interpret due to reduced signal-to-noise ratios, mainly due to dilution with unreacted material and reduced amounts of CSHs present. Exotherms at  $\sim 800^\circ$ ,  $\sim 861^\circ$  and  $\sim 909^\circ\text{C}$  are, however, evident. In this instance, use was also made of the 1st deriv. DTA curve, which revealed a steplike unevenness in the vicinity of  $\sim 900^\circ\text{C}$  and, thus, also confirmed the presence of another exotherm.

*Example 4:* The high temperature region for the sample prepared with 24% MK as cement replacement is shown in Fig. 6 and is clearly different from the previous sample prepared with 24% MK as quartz

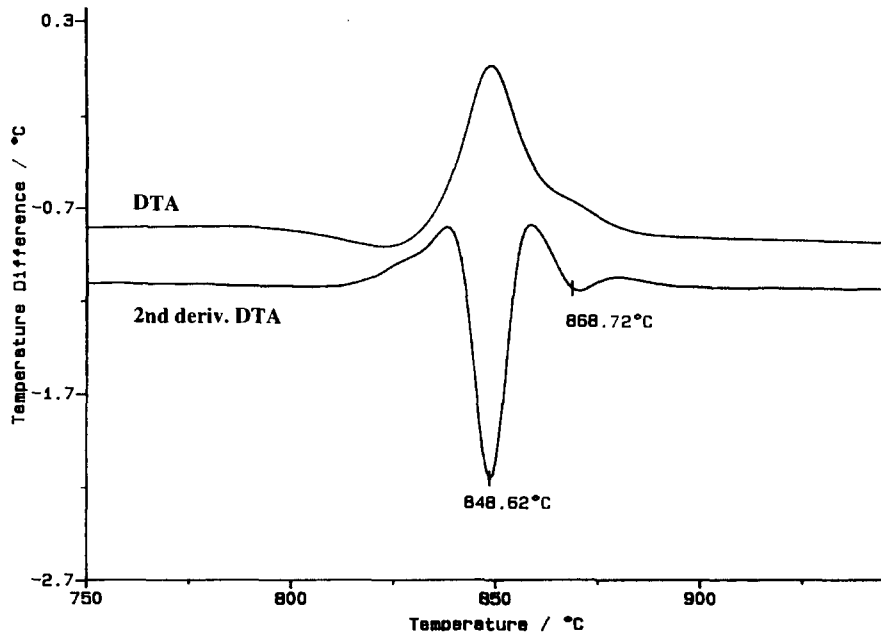


Fig. 3. DTA and 2nd deriv. DTA curves of autoclaved cement-quartz paste with no MK addition.

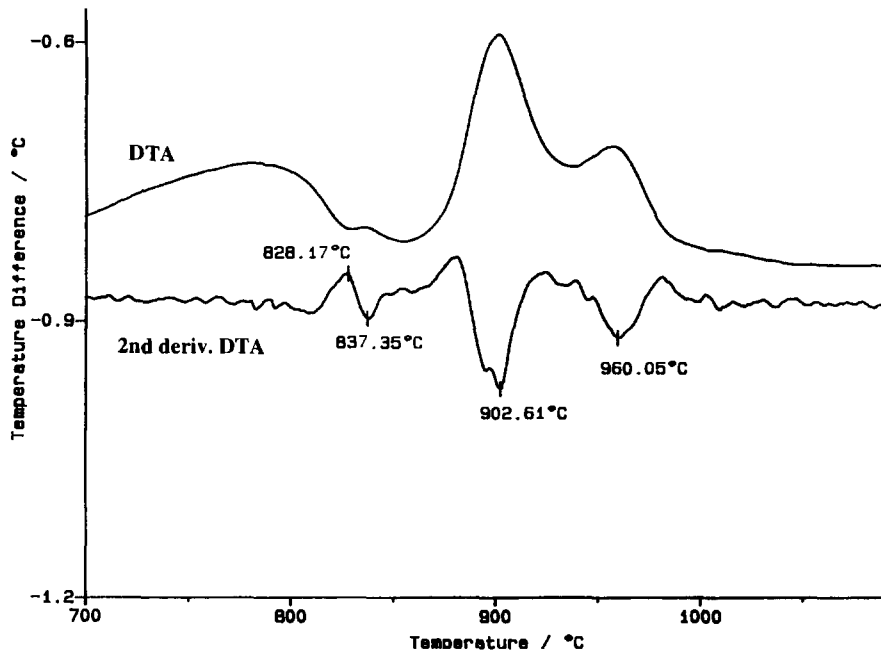


Fig. 4. DTA and 2nd deriv. DTA curves of autoclaved cement-quartz-MK paste when MK was introduced at 12% as quartz replacement.

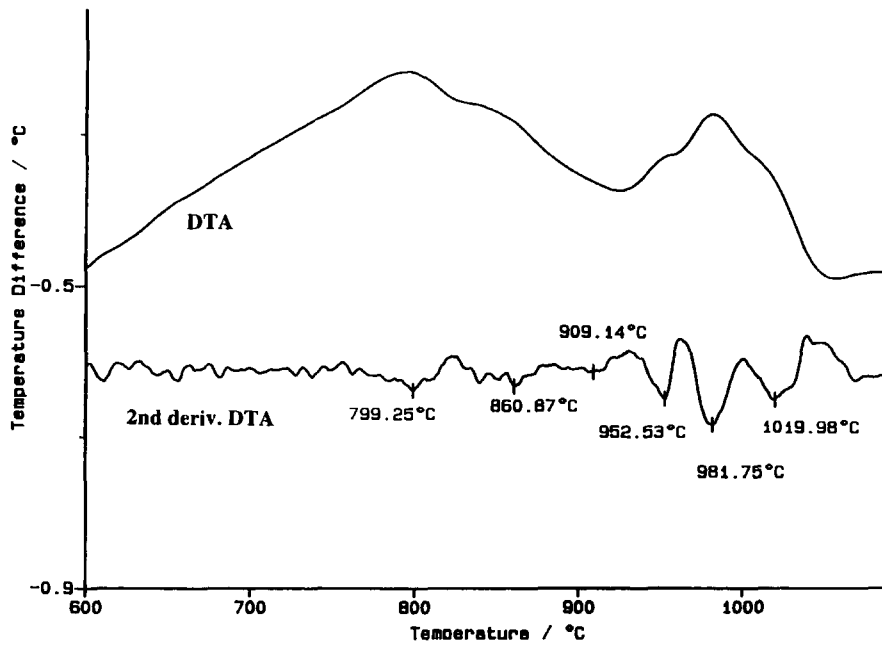


Fig. 5. DTA and 2nd deriv. DTA curves of autoclaved cement–quartz–MK paste when MK was introduced at 24% as quartz replacement.

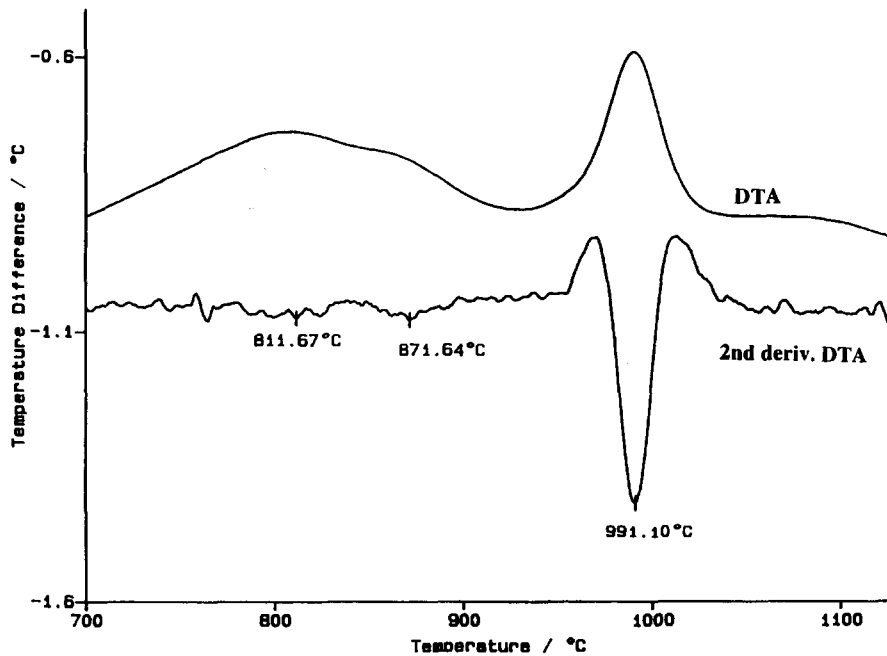


Fig. 6. DTA and 2nd deriv. DTA curves of autoclaved cement–quartz–MK paste when MK was introduced at 24% as cement replacement.

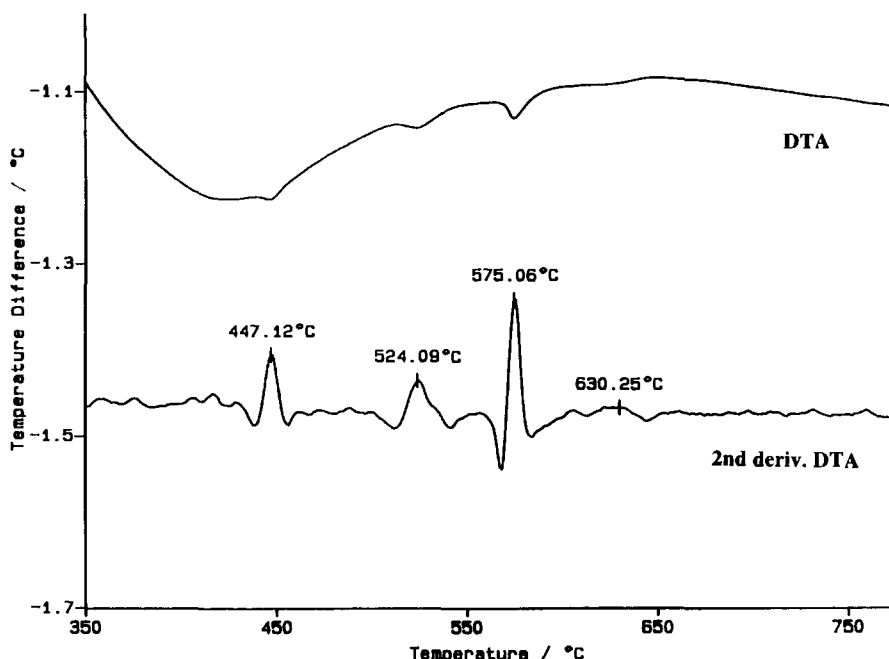


Fig. 7. DTA and 2nd deriv. DTA curves of autoclaved cement-quartz-MK paste when MK was introduced at 18.25% as quartz replacement.

replacement. The most prominent feature is the exotherm at  $\sim 991^{\circ}\text{C}$ . Additionally, two broad exotherms are evident at  $\sim 812^{\circ}$  and  $\sim 872^{\circ}\text{C}$ , no other effects were apparent. This result agrees well with XRD analysis, which indicated traces of hydrogarnet and reduced amounts of CSH, while the  $11\text{ \AA}$   $d$ -spacing of tobermorite was no longer evident, explaining the absence of an exotherm at  $\sim 900^{\circ}\text{C}$  due to Al-substituted tobermorite.

*Example 5:* The 2nd deriv. DTA curve was also useful for detecting small endothermic deflections. In Fig. 7, the endotherm due to portlandite is hardly discernible on the DTA curve, while the 2nd deriv. DTA curve clearly defines this endotherm. A very mild endothermic deflection is also apparent at  $\sim 630^{\circ}\text{C}$ , and has been associated with the CSHs [14]. Endotherms at  $\sim 524^{\circ}$  and  $\sim 575^{\circ}\text{C}$  are apparent on the DTA curve and well-defined by the 2nd deriv. DTA curve.

Table 1. provides a summary of exotherms and endotherms for all samples as determined by employing the 2nd deriv. DTA curve. The onset of unreacted MK detected from our previous findings [7], and the presence of the  $11\text{ \AA}$  peak due to tobermorite from XRD have also been included.

From Table 1. the following trends are apparent:

- The apparent shift to the  $\sim 900\text{--}1000^{\circ}\text{C}$  region, in both series of samples, virtually coincides with the presence of unreacted MK.
- When MK was introduced as quartz replacement, more “lime”-containing phases were formed, as indicated by multiple exotherms above  $\sim 800^{\circ}\text{C}$  due to CSHs and hydrogarnet, in addition to the presence of endotherms due to CH and  $\alpha\text{-C}_2\text{SH}$ .
- When MK was introduced as cement replacement, progressively less CSHs and hydrogarnet were formed, while the amount of unreacted material increased. This is clearly evident from the reduced number of exotherms present above  $\sim 800^{\circ}\text{C}$  and the reduction of other lime-containing phases such as CH and  $\alpha\text{-C}_2\text{SH}$ .

It is interesting to note that, in samples containing unreacted MK the exotherm at  $\sim 1000^{\circ}\text{C}$  appeared at different temperatures due to the mullite transformation. With the exception of samples with MK additions of 30.5%, used as cement replacement, this exotherm appeared at  $\sim 1020^{\circ}\text{C}$  for quartz replacement samples and at  $\sim 990^{\circ}\text{C}$  for cement replacement samples. The

Table 1  
Results from the 2nd deriv. DTA curve of autoclaved cement-quartz-MK pastes when MK was introduced as quartz (Q) and as cement (C) replacement, respectively. (Additional endotherms at  $\sim 130^\circ$ ,  $\sim 200^\circ$  and  $\sim 360^\circ\text{C}$  have been explained in the text.)

% MK introduced as Q or C replacement	11 Å peak present	Unreacted MK detected	$\uparrow^a$ ( $\sim^\circ\text{C}$ )	$\uparrow^a$ ( $\sim^\circ\text{C}$ )	$\uparrow^a$ ( $\sim^\circ\text{C}$ )	$\uparrow^a$ ( $\sim^\circ\text{C}$ )	$\uparrow^a$ ( $\sim^\circ\text{C}$ )	$\uparrow^b$ ( $\sim 445^\circ\text{C}$ )	$\uparrow^b$ ( $\sim 525^\circ\text{C}$ )	$\uparrow^b$ ( $\sim 630\text{--}640^\circ\text{C}$ )
0-Q	{✓} <sup>c</sup>	X	849	868				{✓} <sup>c</sup> tr <sup>e</sup>	X <sup>d</sup>	X <sup>d</sup>
6-Q	{✓} <sup>c</sup>	X	845	873	893	944		{✓} <sup>c</sup> tr <sup>e</sup>	X <sup>d</sup>	{✓} <sup>c</sup> tr <sup>e</sup>
12-Q	{✓} <sup>c</sup>	X	837		903	961		{✓} <sup>c</sup>	X <sup>d</sup>	{✓} <sup>c</sup>
18.25-Q	{✓} <sup>c</sup>	X	836		905	947	982	{✓} <sup>c</sup>	{✓} <sup>c</sup>	{✓} <sup>c</sup> tr <sup>e</sup>
24-Q	{✓} <sup>c</sup>	{✓} <sup>c</sup>	799	861	909	953	1019	{✓} <sup>c</sup>	{✓} <sup>c</sup>	{✓} <sup>c</sup> tr <sup>e</sup>
30.5-Q	X	{✓} <sup>c</sup>	794	859		951	1023	{✓} <sup>c</sup>	{✓} <sup>c</sup>	{✓} <sup>c</sup> tr <sup>e</sup>
6-C	{✓} <sup>c</sup>	X	842		868	948		{✓} <sup>c</sup> tr <sup>e</sup>	X <sup>d</sup>	{✓} <sup>c</sup> tr <sup>e</sup>
12-C	{✓} <sup>c</sup>	X	832		896	966		{✓} <sup>c</sup> tr <sup>e</sup>	X <sup>d</sup>	{✓} <sup>c</sup> tr <sup>e</sup>
18.25-C	{✓} <sup>c</sup>	{✓} <sup>c</sup>	799	865	905	955	994	{✓} <sup>c</sup>	{✓} <sup>c</sup>	{✓} <sup>c</sup>
24-C	X	{✓} <sup>c</sup>	811	872		991		{✓} <sup>c</sup>	{✓} <sup>c</sup>	{✓} <sup>c</sup>
30.5-C	X	{✓} <sup>c</sup>				984		{✓} <sup>c</sup>	X <sup>d</sup>	{✓} <sup>c</sup>

<sup>a</sup> Approximate exotherm temperature.

<sup>b</sup> Endotherm, approximate temperature indicated in brackets.

<sup>c</sup> Present.

<sup>d</sup> Absent.

<sup>e</sup> Trace, indicating that the endotherm was very weak.



shift in peak temperature is significant and suggests the following:

- (a) Unreacted MK may have undergone modifications under autoclaving conditions. These modifications may have been different depending on the environment of the surrounding matrix in addition to the relative amounts of unreacted MK present.
- (b) It is known that the intensity and the position of this exothermic peak are sensitive to the presence of chemical impurities, even when introduced in very small amounts [15]. Serry et al. have reported solid-state reactions between lime and MK, leading to the formation of compounds such as wollastonite, gehlenite and anorthite [16]. As all samples of the present investigation contained unreacted cement, determined by XRD, it is possible that its presence and the presence of other transformation products behaved as mineralizers or catalysts and/or participated in solid-state reactions.

There may, of course, be other reasons for the differences noted. We are currently undertaking a more detailed investigation of MK in autoclaved systems which is expected to provide more insight.

#### 4. Conclusion

From this investigation, we conclude the following:

1. The second-derivative differential thermal curve has been successfully employed in the detection of overlapping peaks and weak endothermic deflection as well as in the determination of peak maxima of overlapping peaks.
2. The second-derivative differential thermal curve has provided more detailed information in the study of autoclaved cement–quartz–MK pastes than the differential thermal curve alone, particularly in the  $\sim 800$ – $1000^\circ\text{C}$  region.
3. With increasing amounts of MK introduced as quartz or as cement replacement, increasing aluminium substitution into the calcium silicate hydrate lattice was evident while hydrogarnet formation increased concurrently.
4. When MK was introduced as quartz replacement, more “lime”-containing phases formed, as indi-

cated by multiple exotherms above  $\sim 800^\circ\text{C}$  due to CSHs and hydrogarnet, in addition to the presence of endotherms due to CH and  $\alpha$ - $\text{C}_2\text{SH}$ .

5. When MK was introduced as cement replacement, progressively less CSHs and hydrogarnet formed, while the amount of unreacted material increased. This was clearly evident from the reduced number of exotherms present above  $\sim 800^\circ\text{C}$  and the reduction of other lime-containing phases such as CH and  $\alpha$ - $\text{C}_2\text{SH}$ .
6. In samples containing unreacted MK, the exotherm at  $\sim 1000^\circ\text{C}$  due to the mullite transformation, appeared at different temperatures. The differences in temperature noted suggest that MK may have undergone modifications during the autoclave process. Alternatively, unreacted cement and/or other transformation products may have acted as mineralizers and/or catalysts or participated in solid-state reactions.

#### Acknowledgements

The continued support given by James Hardie and Coy Pty Limited of Australia to this project is gratefully acknowledged. Special thanks to J. Guerbois from the Materials Science Department at UTS and N.G. Buckman from TA Instruments for useful discussions.

#### References

- [1] J. Ambroise, S. Maximilien, J. Pera, *Adv. Cem. Bas. Mat.* 1 (1992) 161.
- [2] D.M. Roy, A.M. Johnson, *Symp. Autoclaved Calcium Silicate Building Products*, Society of Chemical Industry, London, 1965, p. 114.
- [3] T. Mitsuda, K. Sasaki, H. Ishida, *J. Amer. Ceram. Soc.* 75 (1992) 1858.
- [4] T. Mitsuda, *Amer. Mineral.* 6 (1970) 143.
- [5] E.R. Cantrill, M.G. Stevens, A. Ray, L. Aldridge, *Thermochim. Acta* 224 (1993) 241.
- [6] A. Ray, E.R. Cantrill, M.G. Stevens, L. Aldridge, *Thermochim. Acta* 250 (1995) 189.
- [7] D.S. Klimesch, A. Ray, *Adv. Cem. Res.*, 1996, in press.
- [8] D.S. Klimesch, A. Ray, *Thermochim. Acta* 289 (1996) 41.
- [9] M. Sakiyama, T. Mitsuda, *Cem. Concr. Res.* 7 (1977) 681.
- [10] G.L. Kalousek, *J. Amer. Ceram. Soc.* 40 (1957) 74.
- [11] D.S. Klimesch, A. Ray, *Adv. Cem. Bas. Mat.*, 1997, in press.
- [12] G.L. Kalousek, *ACI J.* (1955) 989.

- [13] V.S. Ramachandran, *Applications of DTA in Cement Chemistry*, Chemical Publishing Company Inc., New York, 1969, p. 99.
- [14] S. Diamond, W.L. Dolch, J.L. White, *Highway Research Record* 62 (1966) 62.
- [15] M. Bulens, B. Delmon, *Clays and Clay Minerals* 25 (1977) 271.
- [16] M.A. Serry, H. El-Didamony, A.A. Abd El-Kader, *Silicates Industriels* 5 (1987) 83.